Structural, dielectric and optical studies of Co doped $Bi_2Fe_4O_9$

A thesis submitted in partial fulfillment for the award of degree in

Master of Science
In
Physics

By

Ms.Tushar Prava Mahanta

Roll No.411PH2098

Under the Guidance of

Prof. Anil K. Singh

Department of Physics

National Institute Of Technology, Rourkela
Rourkela- 769008, Odisha, India
Academic year: 2011-2013

Declaration

I hereby declare that the project work entitled **"Structural, dielectric and optical studies of 20% Co-doped $Bi_2Fe_4O_9$"** submitted to National Institute of Technology, Rourkela, is the record of an original work done by me under the guidance of Dr. Anil K. Singh, Assistant Professor, NIT Rourkela, and this project work has not performed the basis for the award of any degree or diploma/associate-ship/fellowship and similar project if any.

NIT, Rourkela

Tushar Prava Mahanta

Roll No:

Acknowledgements

I owe a debt of gratitude to Prof. Sunil Kumar Sarangi, The Director, NIT, Rourkela for his vision and foresight of this One year Project which has immensely helped all of us to get a flavor and feel of research.

I'd also like to take this opportunity to express appreciation towards our Guide Prof. Anil Kumar Singh for his continuous advice, support. His valuable guidance and suggestions helped me a lot to carry out this project.

I am also very thankful to my lab mates Smita Swain, Sangeeta Ghatuary and all my batch mates for their support and affection.

Last but not the least I would like to thank my parents and all my family members for their support, blessings, encouragement and everything.

CERTIFICATE

This is to certify that the thesis entitled **"Structural, dielectric and optical studies of 20% Co-doped $Bi_2Fe_4O_9$"** submitted by **Tushar Prava Mahanta** bearing **Roll No.-411PH2098** in partial fulfillment of the requirements for the award of degree of Master of Science in Physics at National Institute of Technology, Rourkela is an authentic work carried out by her under my supervision. To the best of my knowledge, the work done in this thesis has not been submitted by any other university/ Institute for the award of any degree or diploma.

Dr. Anil K. Singh
Assistant Professor
National Institute of Technology
Rourkela
Date:

Abstract

The crystal structure, surface morphology, dielectric and optical properties of $Bi_2Fe_4O_9$ and 20% Co-doped $Bi_2Fe_4O_9$ is analysed and compared. $Bi_2Fe_4O_9$ and $Bi_2Fe_3CoO_9$ were prepared by solid state reaction route at 850 ºC. Using X- ray diffraction technique, lattice parameters of $Bi_2Fe_4O_9$ are found to be a= 7.96 Å, b= 9.12 Å, and c= 5.26 Å which is in agreement with previous reports. A comparison of SEM pictures depicts more porosity in $Bi_2Fe_3CoO_9$ as comparison to $Bi_2Fe_4O_9$. UV visible spectroscopy confirms the increased band gap in $Bi_2Fe_3CoO_9$ as comparison to $Bi_2Fe_4O_9$. For a particular frequency and temperature dielectric constant of $Bi_2Fe_3CoO_9$ is less than $Bi_2Fe_4O_9$.

INDEX

1. INTRODUCTION

1.1 Magnetism and its classification

Magnetism is an intrinsic property of a material for which it responds to an external magnetic field. In general magnetism arises due to two sources:

1. Electrical current or moving charges.

2. Spin magnetic moment.

Magnetic susceptibility indicates the degree of magnetization. Depending upon the nature of response shown by magnetic materials and the orientation of magnetic dipoles they are classified into following categories:

(a) Diamagnetism

It is an intrinsic property of all magnetic materials and it is the tendency to oppose applied magnetic field i.e. in a strong magnetic field they acquire very weak magnetization in the direction opposite to the applied field. So these substances have negative susceptibility which does not depend on temperature.

(b) Paramagnetism

Magnetic dipoles of paramagnetic substances are randomly oriented so that there is no resultant magnetization. When the material is exposed to an external magnetic field dipoles tend to orient themselves along the direction of applied field and produce a net magnetization. Magnetic susceptibility of paramagnetic substances is a small positive quantity which is inversely proportional to temperature.

Example: Cr, $CuSO_4$, Pt, Al etc.

(c) Ferromagnetism

It is a property of some magnetic materials which exhibit a strong magnetization even in the absence of any external applied field. The behaviour of retaining some magnetization in the absence of applied magnetic field is called hysteresis and the curve between magnetization and applied magnetic field is called hysteresis loop. Some important terms are shown with the help of hysteresis loop.

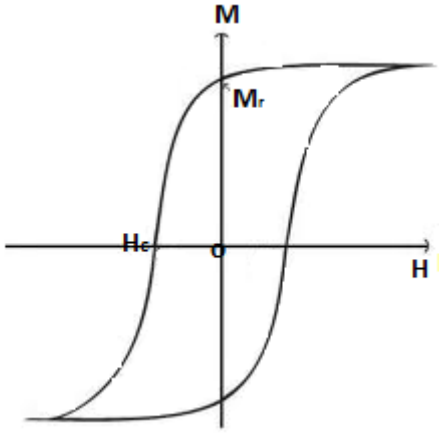

Fig.1. Hysteresis loop of ferromagnetic material (M – Magnetization, H- Applied magnetic field, M_r – Retentivity, H_c –Coercivity)

They have a large positive magnetic susceptibility which depends on Curie temperature. Above certain temperature (i.e. curie temp.) ferromagnetic materials changes into paramagnetic which can be explained with the concept of magnetic domain.

Example: Fe, Co, Ni etc.

(d) Antiferromagnetism

There is an anti-parallel alignment of magnetic spins in the neighbouring atoms. The anti parallel spins become independent and become paramagnetic after a certain temperature known as Nèel temperature. Magnetic susceptibility of anti-ferromagnetic material is directly proportional to temperature.

Example: MnO, MnS, FeO, NiO etc.

(e) Ferrimagnetism

It is a special case of anti-ferromagnetism where they have spins aligned in opposite direction with unequal magnetic moments, as a result there is a large net magnetization.

Magnetic spin alignment of all types of magnetic materials is shown below:

Para magnetism	Ferromagnetism	Anti-ferromagnetism	Ferrimagnetisms
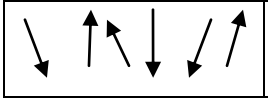	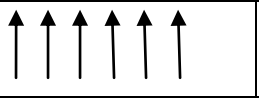	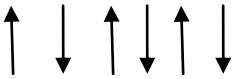	

Fig.2.Spin alignment in different types of magnetic materials

Change in susceptibility with temperature in different types of magnetic materials are shown below

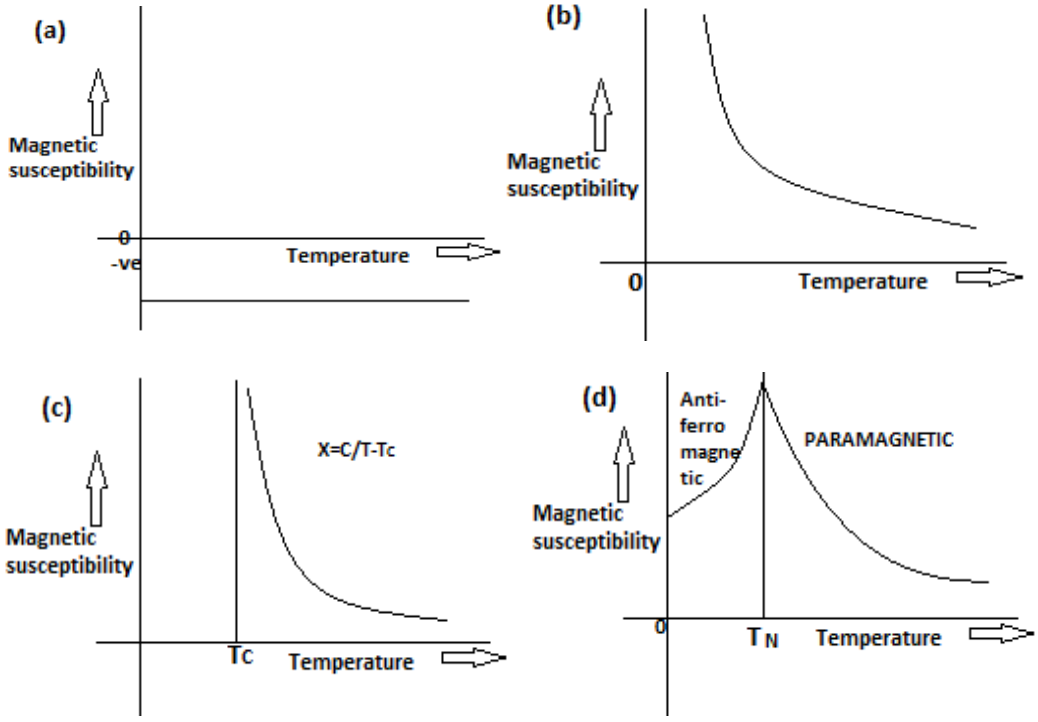

Fig.3. Magnetic susceptibility as a function of temperature in (a) Diamagnetism (b)Paramagnetism (c) Ferromagnetism (d) Antiferromagnetism (Ref. **1**)

1.2. Ferroelectricity

A ferroelectric material exhibits an electric dipole moment even in the absence of any external electric field. Like ferromagnetic materials in ferroelectric materials also the plot of polarizations verses electric field shows a hysteresis loop. Ferroelectricity usually disappears above a certain temperature called the transition temperature and shows paraelectricity.

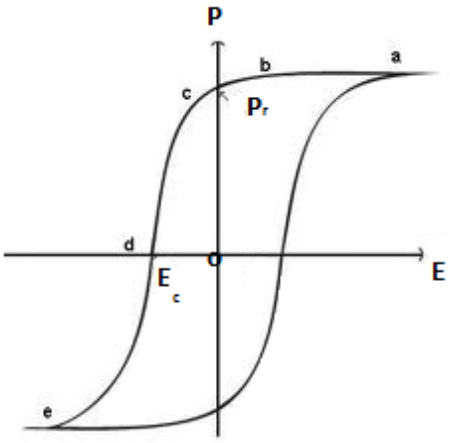

Fig.4.Hysteresis loop in ferroelectric material **(P_R-** Retentive polarization, **E_C** – Coercive field, E - Applied electric field,P – Polarization)

Generally ferroelectric materials have a perovskite crystal structure. The spontaneous polarization generates because of the crystal distortion.

Examples: Barium titanate ($BaTiO_3$), lead zirconium titanate (PZT) etc.

1.3. Ferroelasticity

Ferroelastic materials develop a spontaneous strain below a certain transition temperature even in the absence of stress. Ferroelasticity arise from a structural phase transition which leads to two possible orientations of states which are equally stable. The states can switch each other in the presence of a very small stress. Ferroelstic property associates with the stress-strain hysteresis.

Example: $BaTiO_3$, $BiVO_4$, Mn_3O_4 etc.

1.4. Multiferroics

Before 19th century electric and magnetic Properties in solids are generally considered independently because of the following reasons:

1. Electrons and ions are responsible for the electric properties, whereas electron spins control magnetic properties.

2. Magnetism originates due to presence of partially filled electrons in *d*- or *f*-sub shell but the origin of electricity is due to the presence of d^0orbital.

The term multiferroic was first introduced by Schemed. Multiferroics defines the materials in which two or three types of ferroic order i.e. ferrelectricity (-anti), ferromagnetism (-anti) and ferroelasticity occurs simultaneously in the same phase.

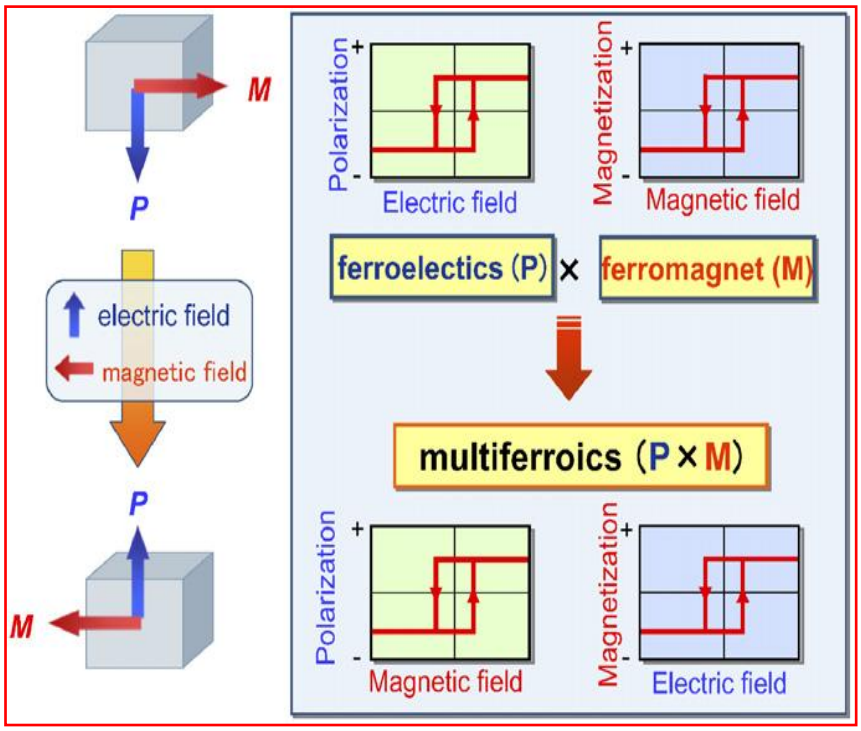

Fig.5. Magneto-electric coupling in multiferroics (Ref.**13**)

The interaction of ferroelectric and magnetic (ferromagnetic or antiferromagnetic) property leads to a phenomenon called Magneto-electric effect, which is the introduction of magnetization by an electric field or electric polarization by a magnetic field. Depending upon the source of magnetic and electric contribution towards the magneto-electric effect multiferroics are classified into two categories.

1.4.1 Type- I Multiferroics

These are the materials in which ferroelectricity and ferromagnetism have different sources and they are independent of each other. For example $BiFeO_3$ which is a multiferroics at room temperature shows a ferroelectric phase transition at 1100 K whereas ferromagnetic transition temperature is 643 K. So the magneto-electric coupling is weak but polarization generated is very high. There are four different subclasses of type-I multiferroics, depending on the mechanism of ferroelectricity in them.

(a) Multiferroic Perovskites

Perovskites structure is most common in ferroelectric materials like $BaTiO_3$. Magnetism needs partially filled d shells whereas electricity is due to empty d-shells. All perovskites contain transition metal ions (Ti^{4+}) with an empty d-shell. The ferroelectricity in these perovskites system is produced by the off-centre shifts of the transition metal ion which forms a strong covalent bond with oxygen. The presence of d-electron somehow suppresses the ferroelectricity which is also called d^0 vs. d^n problem. So the magneto-electric coupling is weak.

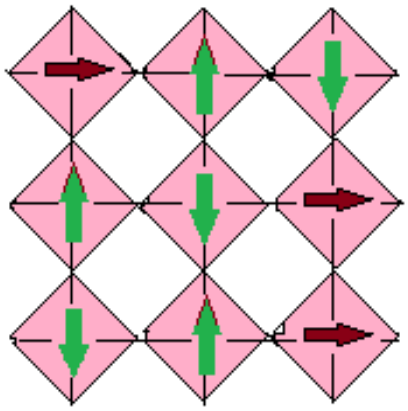

Fig.6. Multiferroic perovskites with ferroelectrically, shifts of electrically active d^0 ions (brown) from the centres of oxygen (pink plaquettes) lead to polarization (along brownarow), coexisting with magnetic order (green arrows). (Ref. **5**)

(b) Ferroelectricity Due To Lone Pairs

In some multiferroics like $BiFeO_3$ and $PbVO_3$, Bi^{3+} and Pb^{2+} plays a major role in the origin of ferroelectricity and in these ions the two outer 6s electrons do not have any contribution in chemical bonds. They are called lone pairs and these are the main source of generating polarization. By ordering these lone pairs along a certain direction we can achive ferroelectricity.

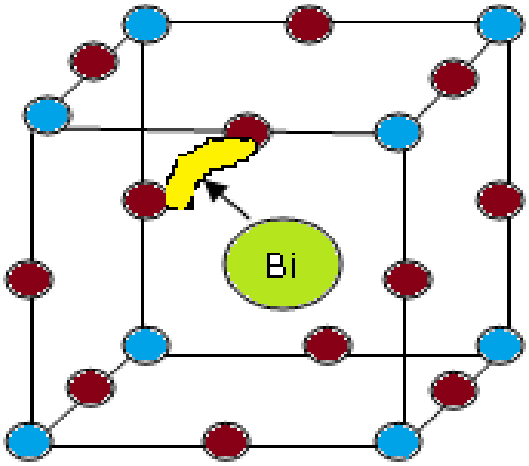

Fig.7. $BiFeO_3$ Multiferroics with ordering of lone pairs (yellow lobes). (Ref. **5**)

(c) Ferroelectricity Due To Charge Ordering

Another mechanism that leads to ferroelectricity in type-1 multiferroics is the charge ordering.Transition metal ions have different valence electrons, so they have different charge.In charge ordered systems,the coexistence of inequivalent sites with different charges with unequal bonds, leads to ferroelectricity.

Examples:$TbMnO_3$ and Nickelates($RNiO_3$)

(d) Geometric Ferroelectricity

In these multiferroics, ferroelectricity is caused by tilting the oxygen octahedron. For example in $YMnO_3$ tilting of MnO_5 block tilt the Y-O bond and form dipoles and they appears two up dipoles and one down dipole so the system becomes ferroelectric.

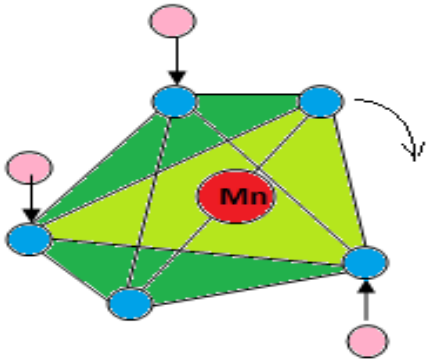

Fig.8. Mechanism of generation of polarization in $YMnO_3$ (Ref. **5**)

1.4.2. Type –II Multiferroics

In this type of multiferroics ferroelectricity exist in a magnetically ordered state i.e. magnetic field can strongly influence the electric polarization. For example, in $TbMnO_3$ magnetic ordering appears at T_{N1} =41 K and T_{N2} =28 K but magnetic structure changes only at 28 K and non-zero electric polarization appears at low temperature phase i.e. at 28K.

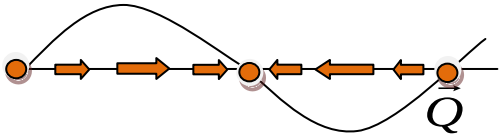

Fig.9. Type-II Multiferroics - Sinusoidal spin density wave(Ref. **5**)

Type –II Multiferroics are divided into two groups depending on the microscopic origin of multiferroicity:

(a) Spiral Type-II Multiferroics

Ferroelectricity appears by combining the spiralling magnetic phase. For example in $TbMnO_3$ below $T_{N1} \approx 41K$ the magnetic spins orients in one direction but the total magnetic moment is zero. Below $T_{N2} \approx 28K$, the Mn spins order and shows a cycloid structure. The polarization which appears in a cycloid spiral structure is given by:

$$\vec{P} \approx \vec{r}_{ij} \times \left[\vec{S}_i \times \vec{S}_j\right] \approx \left[\vec{Q} \times \vec{e}\right]$$

Where $\vec{r}_{ij}$ the vector connecting neighbouring spins $\vec{S}_i$ and $\vec{S}_j$. $\vec{Q}$ is the wave vector describing the spiral and $\vec{e}$ is the spin rotation axis. Above equation shows that mechanism of polarization is connected to spin-orbit interaction. Magnetic frustration is the source of magnetic ordering. The effect of external field on a cycloid is similar to spin-flop transition in anti-ferromagnetism i.e. when a magnetic field is applied the plane of the cycloid tilt by 90º, and so polarization generates.

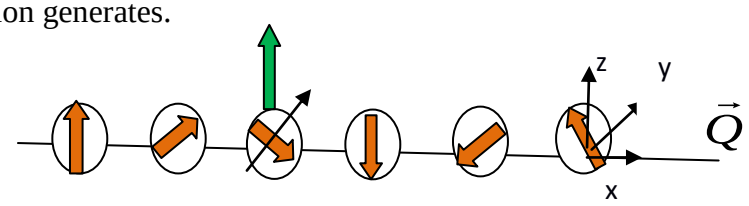

Fig.10. Cycloid spiral structure with wave vector $\vec{Q}$ (Ref. **5**)

Examples: $TbMnO_3$, NiV_2O_8 and $MnWO_4$

(b) Type –II Multiferroics with collinear magnetic structures

These are the multiferroics in which ferroelectricity appears in collinear magnetic structures i.e. all magnetic moments align along a particular direction without the involvement of spin-orbit interaction. At high temperature the ionic chain of these types of multiferroics maintain inversion symmetry, so the polarization is zero.

Magnetic ordering breaks the inversion symmetry, so the Ferro- and anti-Ferro bonds get distorted and we end up the situation (as shown in fig.) of the material as ferroelectric.

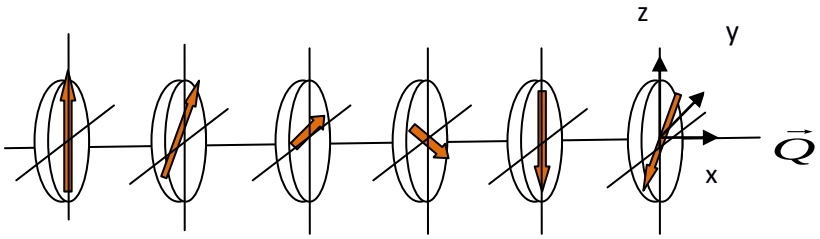

Fig.11. Type-II Multiferroics with collinear magnetic structures-Spins are rotating in a plane perpendicular to $\vec{Q}$ with broken inversion symmetry (Ref. **5**)

Example**:** Ca_3CoMnO_6 etc.

1.5. Magnetic Frustration

Magnetic frustration is an important feature in antiferromagnetic materials which generates from the arrangement of spins. For example in a triangle shape anti ferromagnetic crystal three spins must reside on the corners with anti-parallel ordering, so as to minimize its interaction energy.

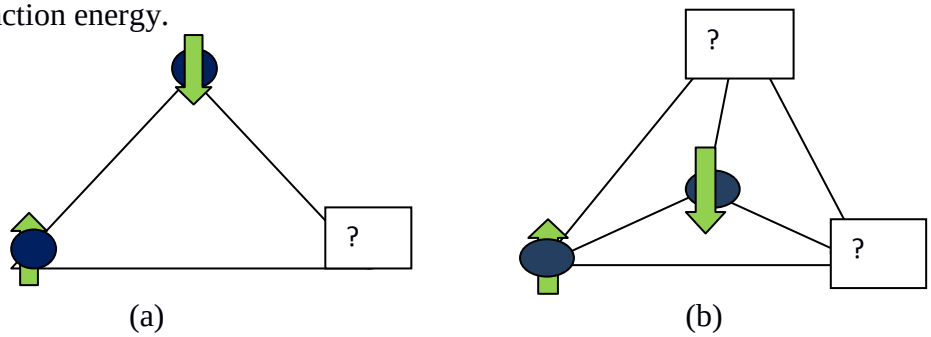

Fig.12.Spin frustration in (a) triangle and (b) tetrahedral crystal structure.

Once the first two spins align anti-parallel the third spin is getting frustrated because of its two possible orientations, spin-up and spin-down. The third spin can't minimize its interaction energy so the state may experience a magnetic frustration. Degree of frustration can be calculated from the relation $f = \theta_{CW} / T_N$, where θ_{CW} and T_N are the curie-Weiss and Nèel temperature respectively. In case if the ratio is greater than 1 the crystal suffers large degrees of magnetic frustration.

2. MOTIVATION

For most of the multiferroics transition temperature is very low (below liquid N_2 temperature). But in case of $Bi_2Fe_4O_9$ the transition temperature is ~265 K which is very near to room temperature. Being a type II multiferroic, magnetoelectric coupling is very strong in $Bi_2Fe_4O_9$. It is also very important to study how the structural, dielectric and optical properties get modified due to doping at Fe site.

3. CRYSTAL AND MAGNETIC STRUCTURE OF $Bi_2Fe_4O_9$

3.1. Crystal structure

From X ray diffraction studies it was found that $Bi_2Fe_4O_9$ has orthorhombic structure. Iron atoms have two different sites which are arranged in tetrahedral and octahedral manner. Bismuth atoms are distributed at the interior of the structure surrounded by oxygen octahedral. The lattice parameters of $Bi_2Fe_4O_9$ are reported to be a=8.0627Å, b=8.5584Å and c=6.0086Å.

3.2. Magnetic structure

$Bi_2Fe_4O_9$ crystals belong to Pbam space group. The compound is paramagnetic at room temperature and undergoes a phase transition at T_N=264 K to anti ferromagnetic state. The frustration parameter i.e. the ratio between paramagnetic temperature and Nèel

temperature was found to be greater than one showing a large degree of frustration. The magnetic moment of the compound was found to be (4.95 ± 0.08) $\mu_{B.}$ The magnetic structure of the compound was shown below:

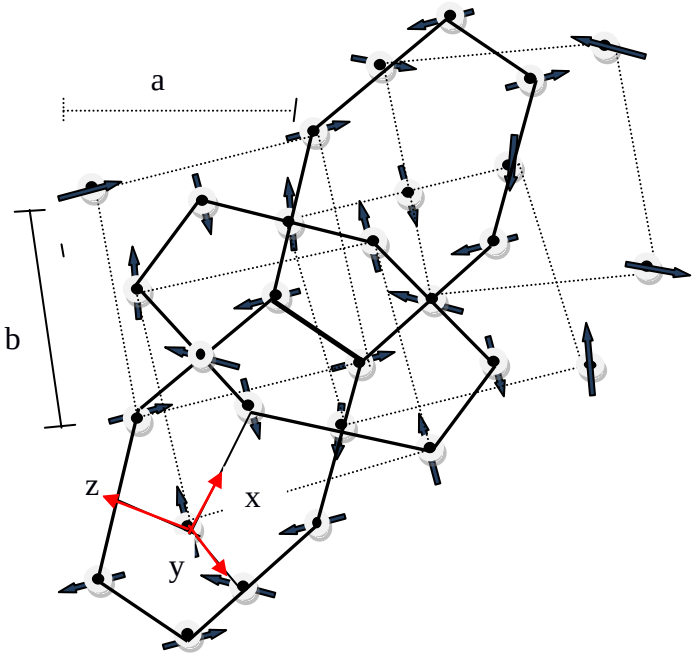

Fig.13.Magnetic structure of $Bi_2Fe_4O_9$ showing pentagonal Cairo lattices (a, b are the lattice parameters).

There are two different sites of four iron atoms in $Bi_2Fe_4O_9$. Fe (1) occupies a tetrahedral position and Fe (2) an octahedral one. Within a layer, each Fe (1) interact with its neighbour Fe (1), via ferromagnetic interaction and with nearest neighbour Fe (2) pair via anti-ferromagnetic interaction. The projections of this lattice along c-axis form a pentagonal lattice with three slightly different bond strengths.

4. PREVIOUS REPORTS

4.1. Substantial magneto-electric coupling near room temperature in $Bi_2Fe_4O_9$

A.K.Singh *et al.*Appl. Phy. Lett, **92**,132910(2008).

This paper gives brief idea on structural and on multiferroic effect in polycrystalline $Bi_2Fe_4O_9$ prepared by solid state reaction technique. Lattice parameters are calculated from Powder diffraction data as a=8.0627Å, b=8.5584Å, and c=6.0086 Å. Polycrystalline $Bi_2Fe_4O_9$ exhibits an antiferromagnetic phase transition at T_N =260K and it contains octahedral and tetrahedral iron sites lead to spin frustration. At room temperature no hysteresis behaviour was identified due to leakage current and P-E loop of the sample was observed below 250K which is close to magnetic phase transition.Significant anomalies in dielectric constant and tangent loss around the anti-ferromagnetic transition temperature T_N=260K shifts to higher temperature with the application of magnetic field.The sample provides a clear evidence for strong coupling of electric polarization and magnetic moments. The non-collinear magnetization due to spin frustration provides a suitable mechanism for the magneto-dielectric effect.

4.2.Magnetic frustration in an iron based Cairo pentagonal lattice

E. Ressouche*et al.* Phys. Rev. Lett. **103**, 267204(2009)

This paper gives brief idea on the crystal and magnetic structure of $Bi_2Fe_4O_9$ prepared by the high temperature solution growth method. From characterization data it was found that above room temperature $Bi_2Fe_4O_9$ obey curie-Weiss law giving a frustration parameter greater than one which suggestslarge degrees of frustration. It has a non-collinear magnetic structure, having a fourfold spin rotations. There are two different sites of four iron atoms in $Bi_2Fe_4O_9$.Fe (1) occupies a tetrahedral position and Fe (2) an octahedral one. Within a layer, there is a ferromagnetic interaction between each tetrahedral iron atoms

and anti-ferromagnetic interaction with nearest octahedral atoms. They form a pentagonal lattice which is also known as Cairo pentagonal lattice with three slightly different bond strengths. The only parameter that varies as a function of the particular values of magnetic moment is the phase angle between the two sites, octahedral and tetrahedral iron.

5. SAMPLE PREPARATION

The sample was prepared by solid state reaction techniquewhich is the most widely used method for the preparation of polycrystalline solid from a mixture of starting materials. Generally Solids do not react together at room temperature over normal time scales so it is necessary to heat them to much higher to 1000 to 1500° C in order for the reaction to occur at an appreciable rate. The factors on which feasibility and rate of a solid state reaction depends includes, reaction condition, structural properties of reactants, surface area of the solids, their reactivity and the thermodynamic free energy change associated with the reaction

SYNTHESIS OF$Bi_2Fe_3CoO_9$

2 g of $Bi_2Fe_3CoO_9$ was synthesized through solid state reaction route using 1.1820g of Bi_2O_3, 0.6076 g of Fe_2O_3 and 0.2016g of Co_3O_4 as precursor.

- It follows the reaction

$$Bi_2O_3 + 1.5Fe_2O_3 + 0.33Co_3O_4 \rightarrow Bi_2Fe_3CoO_9$$

- The mixture is ground for 3 hours.

CALCULATION

Chemical Reaction

$$Bi_2O_3 + 2(1-x)Fe_2O_3 + 2(x)Co_3O_4 \rightarrow Bi_2Fe_{4(1-x)}Co_{4x}O_9$$

Molar mass of Bi =208.98 g/mol

Molar mass of Fe =55.81 g/mol

Molar mass of Co=58.93 g/mol

Molar mass of Bi_2O_3 =465.93 g/mol

Molar mass of Fe_2O_3 = 159.67 g/mol

Molar mass of Co_3O_4 =165.83 g/mol

For 20% of cobalt doping the Reaction will be

$$Bi_2O_3 + 1.5Fe_2O_3 + 0.33Co_3O_4 \rightarrow Bi_2Fe_3CoO_9$$

M [$Bi_2Fe_3CoO_9$] =788.4245 g/mol

For 2g of$Bi_2Fe_3CoO_9$ sample

Bi_2O_3 Required $= 465.959/(788.4245 \times 2) = 1.1820g$

Fe_2O_3 Required $= [(159.6882 \times 1.5)/788.4245] \times 2 = 0.6076g$

Co_3O_4 Required $= [(240.7972 \times 0.331)/788.4245] \times 2 = 0.2016g$

Flow Chart:-

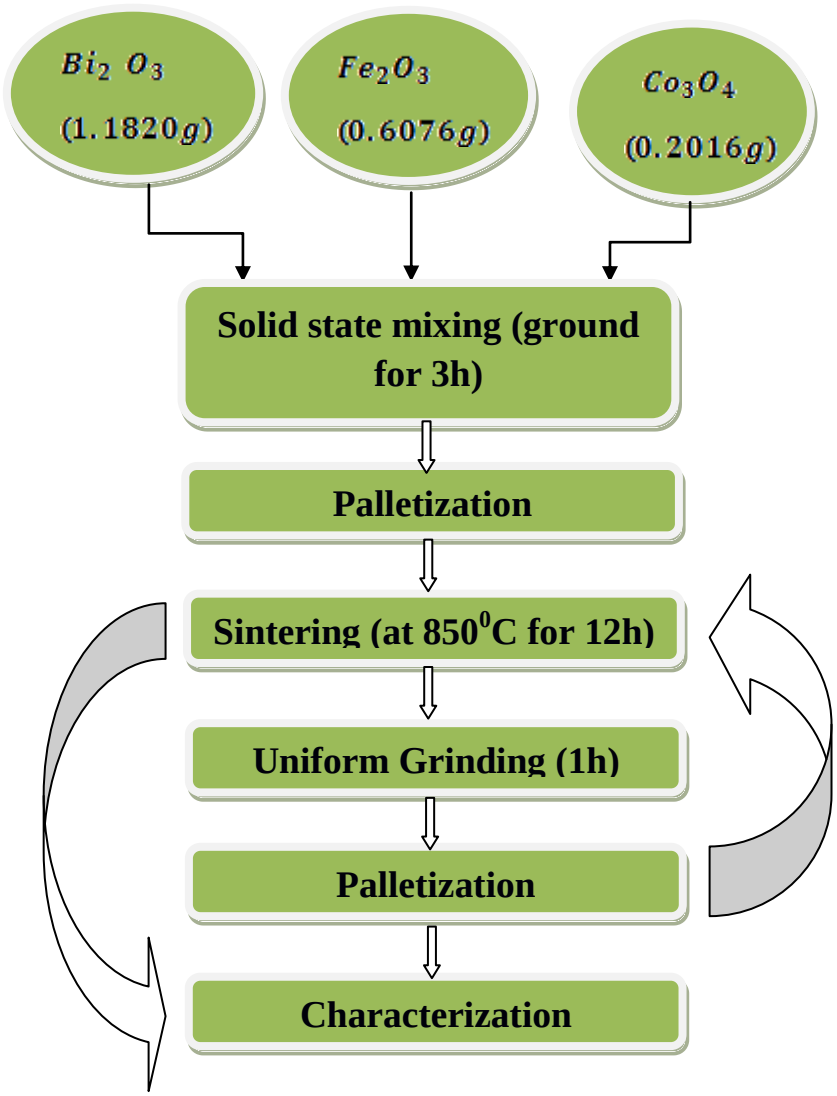

Fig.14.Flow chart for synthesis of $Bi_2Fe_3CoO_9$

Palletization

The grinded powders were pressed using a Hydrolyic Press at 5 torr pressure and pallets were made using dye.

Sintering

After palletization all pellets were kept into the furnace at 850˚C for 12 hrs.keeping ramping rate at 5˚ C/min. Sintered pellets were again ground for half an hour and pellets were made from it. Then samples were characterized by XRD, SEM and Dielectric constant measurement.

6. CHARACTERIZATION TECHNIQUES

(i) X-Ray Diffraction

The idea that crystals could be used as a diffraction grating for X-rays arose in 1912. **X-ray diffraction** is a technique used for determining the crystallite structure of a crystal. Crystals are considered to be regular arrays of atoms. The interaction of x-ray with the electrons can be understood using elastic scattering. A regular array of atoms produces a regular array of scatter waves.

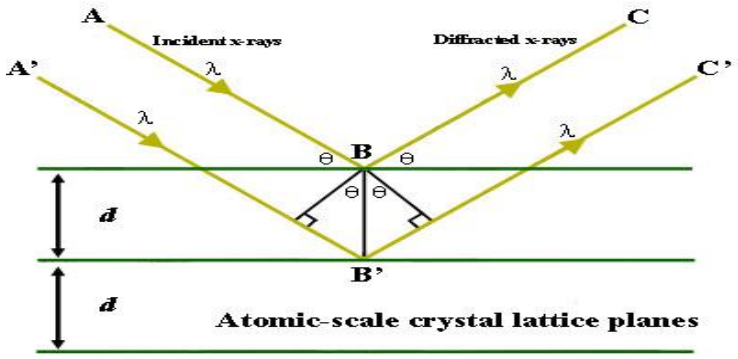

Fig.15.Bragg's law of x-ray Diffraction (Ref.**14**)

A perceptive understanding of X-ray diffraction can be obtained from the Bragg model of diffraction. In which, X-rays scattered from adjacent planes of the crystal will combine constructively when the phase shift is an integral multiple (*n*) of the X-ray wavelength λ and is explained by Bragg's law

$$2d\sin\theta = n\lambda$$

Where *d* is the spacing between the diffracting planes, θ is the incident angle, *n* is an integer, and λ is the wavelength of the x-ray beam. These specific directions appear as spots ondiffraction pattern called reflections. Thus, X-ray diffraction results from the X-ray impinging on a regular array of atoms within the crystal gives the real x-ray diffraction graph.

An x-ray measurement instrument basically consists of an x-ray source, filter, goniometer, detector and a collimator. X-rays are generated by a cathode ray tube and filtered to produce a monochromatic radiation which is collimated to concentrate, and directed toward the sample. Then the diffracted rays are collected which gives the information about the crystallite size of the crystal.

(ii) Scanning Electron Microscope

A scanning electron microscope produces raster images of a sample by scanning it with a focussed beam of electrons. The interaction of electrons with electrons in the sample produces various signals that can be detected and that contain information about the sample's surface texture and chemical composition.

When electron beam scanned over the specimen a signal is produced due to scattering.

- Elastic Scattering

When a beam of electron passes close to the nucleus, it may be attracted by the nucleus or may deflect at some angle losing a small fraction of their kinetic energy. Many of those which are deflected through very large angles ($>90^{o}$) re-emerge from the surface of specimen with a very high energy. These are more often called "backscattered electrons" (BSE).

- Inelastic Scattering

Some of the incident electrons will interact with the orbiting shell electrons, losing a large proportion of their energy. This results into production of phonon, secondary electrons and auger electrons.

Important Parts of SEM:

- Electron gun
- Electron Lens
- Electron detector

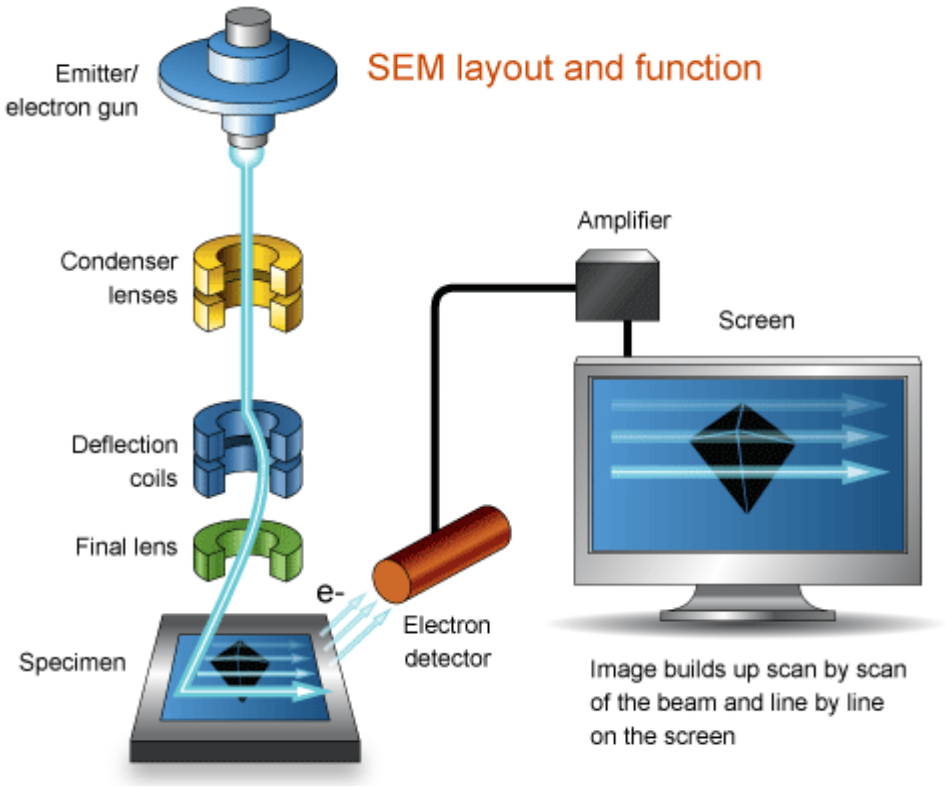

Fig.16. Layout of Scanning electron Microscope (Ref.**15**)

Electron gun helps in producing accelerated electrons with a velocity of a fraction of the speed of light. The electron detector is in the form of p-n junction. When it hit by the energetic backscattered electrons from our specimen inelastic scattering occurs in the semiconductor. This moves electrons into conduction band where they are free to move about. The resulting holes left in the valence band can also move about. Normally these free electron/hole pairs would recombine, but if a small potential is applied across the wafer, they are swept apart resulting in a small electric current. A very sensitive amplifier is needed to produce a signal large enough to vary the intensity of SEM display screen.

(iii) Dielectric Spectroscopy

Dielectric spectroscopy (also known as impedance spectroscopy), measures the dielectric properties of a material as a function of frequency. Impedance is the opposition to the flow of alternating current (A.C.) in a complex system. It is based on the interaction of an external field with the electric dipole moment of the sample, often expressed by permittivity. This technique measures the impedance of a system over a range of frequencies, and therefore the frequency response of the system, including the energy storage and dissipation properties, is revealed.

Tangent loss is a parameter of a dielectric material that measures its dissipation of electromagnetic energy. The term refers to the tangent of the angle in a complex plane between the resistive (lossy) component of an electromagnetic field and its reactive (lossless) component. Permittivity can be expressed as a complex quantity with a real and an imaginary part.

$$\in = \in' - j \in''$$

Suppose we have an electromagnetic wave function, $E = E_o e^{j\omega t}$

The tangent loss is then defined as the ratio (or angle in a complex plane) of the lossy reaction to the electric field E in the curl equation to the lossless reaction:

$$\tan\delta = (\omega \in'' + \sigma) / \omega \in'$$

The loss is very small for a dielectrics with an angle<<1.

(iv) UV-Visible Spectroscopy

It is a type of absorption or reflectance spectroscopy in the ultraviolet-visible region. This means it uses light in the visible, near-UV and near-infrared ranges of electromagnetic radiation.

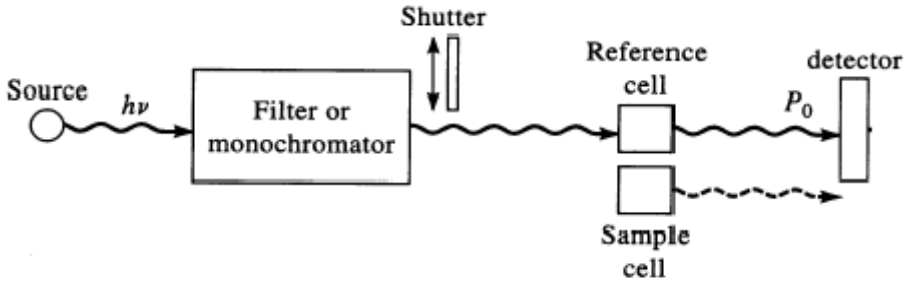

Fig.17.Ray diagram of UV-Visible Spectrometer (Ref.**16**)

An UV-Visible Spectrometer consists of a monochromatic source of light, sample holder and a detector to analyse the absorbed or reflected light. Molecules undergo electronic transitions in the visible or near UV range of electromagnetic spectrum. Molecules containing valence electrons absorbs the energy in the form of ultraviolet or visible light to excite these electrons to higher excited molecular orbital. The more easily excited the electrons can absorb a light of longer wavelength. Measurement of transmittance and absorbance is done by using Beer-Lamberts law. Absorbance of the sample is defined as, $A = -\log_{10}(I / I_o) = \alpha l$, where α is the absorbance coefficient.

7. RESULT AND DISCUSSION

(i) X-Ray Analysis

In x-ray diffraction, the samples are scanned in a continuous mode from 20˚-80˚ with a scanning rate of 2˚ per minute. XRD pattern of pure $Bi_2Fe_4O_9$ sintered at 850˚c is shown in the **fig.18.** The prominent peaks in the plot are indexed to various [h k l] planes of $Bi_2Fe_4O_9$ using JCPDFWIN. The x-ray plot for 20% cobalt doped $Bi_2Fe_4O_9$ was shown in the **fig 19**.

Most of the major peaks are in accordance with $Bi_2Fe_4O_9$. Other than major peaks few other peaks may be attributed for the following reasons.

(i) Reaction with the alumina crucible.

(ii) At high temperature, there is always a possibility of loss of cobalt from cobalt oxide that increases the temperature, which may have the contribution to the extra low Intensity peaks.

From literature survey I came to know the value of lattice parameters a, b, and c as 7.965Å, 8.440 Å and 5.994 Å respectively. Taking [h k l] values from the XRD plot lattice parameters are calculated. For orthorhombic structures the relation between [h k l] and a, b, c is given by

$$\frac{1}{d^2} = \frac{h^2}{a^2} + \frac{k^2}{b^2} + \frac{l^2}{c^2}.$$

By solving this equation the values of a, b, and c are found to be 7.96 Å, 9.12 Å, and 5.26 Å respectively. Crystallite size is also calculated using Scherer's formula,

$$D = \frac{0 \cdot 9\lambda}{\beta \cos\theta}$$

The crystallite size of $Bi_2Fe_3CoO_9$ (51.91 nm) is found to be more than $Bi_2Fe_4O_9$ (51.62nm).

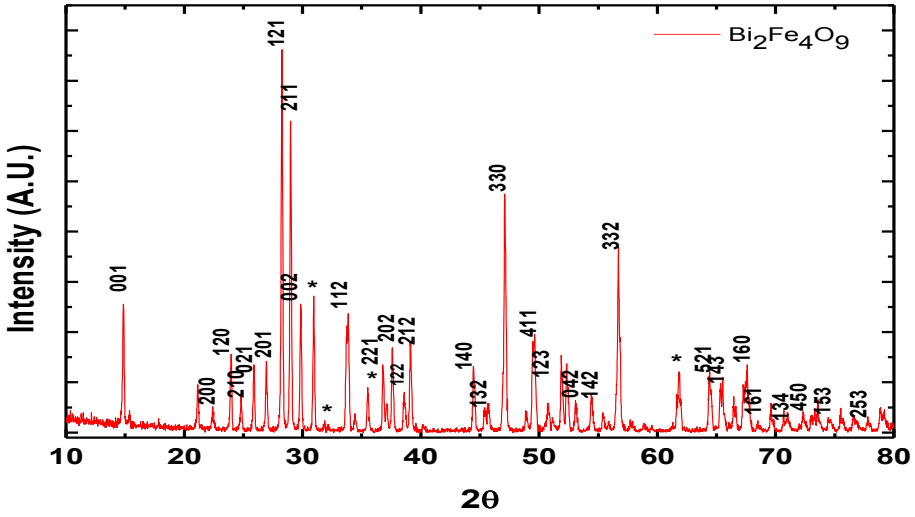

Fig.18.X-Ray Diffraction of $Bi_2Fe_4O_9$

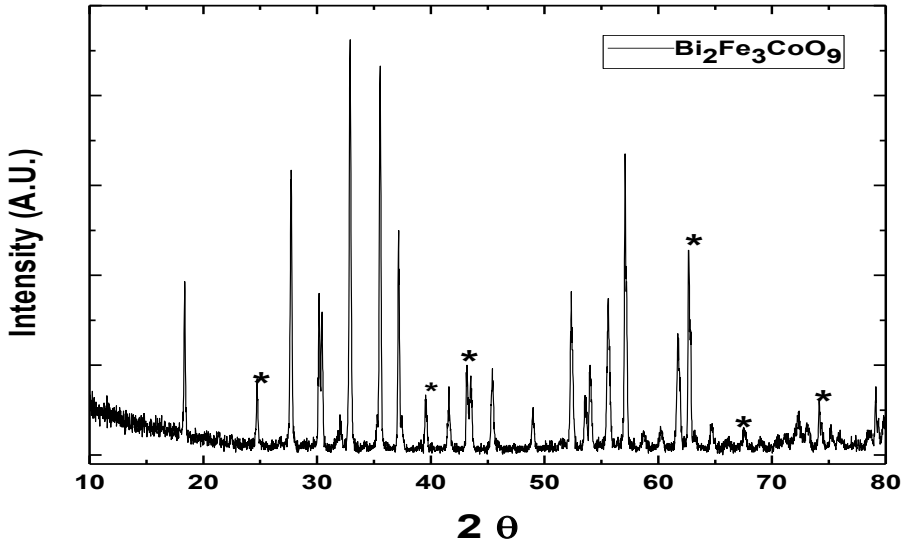

Fig.19. x-ray diffraction plot of 20% Co-doped $Bi_2Fe_4O_9$.

(ii) SEM Analysis

The Scanning electron microscope images of $Bi_2Fe_4O_9$ and 20% cobalt doped $Bi_2Fe_4O_9$ are shown in the **fig.20** and **fig .21** respectively. Comparison of both the images shows the following results.

(i) Density of $Bi_2Fe_4O_9$ is more than the $Bi_2Fe_3CoO_9$.

(ii) The grain size similarity and separation between them shows more equal in Bi2Fe3CoO9 than $Bi_2Fe_4O_9$.

(iii) $Bi_2Fe_3CoO_9$shows more porosity than the $Bi_2Fe_4O_9$.

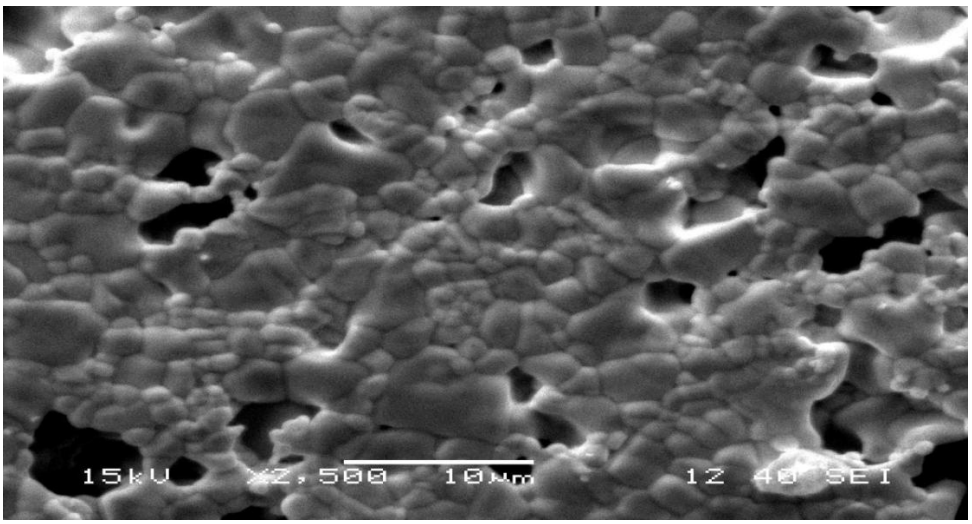

Fig.20.SEM image of$Bi_2Fe_4O_9$

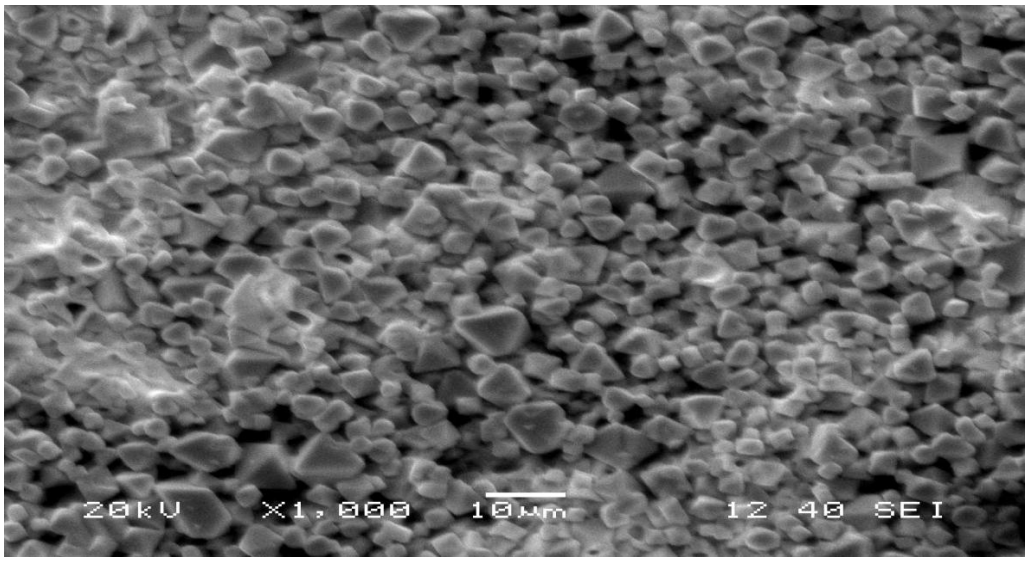

Fig.21.SEM image of Co-doped $Bi_2Fe_4O_9$

(iii) Dielectric Spectroscopy Analysis

The dielectric measurement as a function of frequency in the range of 1 Hz to 1 kHz is done. Fig 22, 23, 24 and 25 shows the variation of tan δ, impedance, and dielectric constant with the frequency respectively for $Bi_2Fe_4O_9$ and $Bi_2Fe_3CoO_9$.

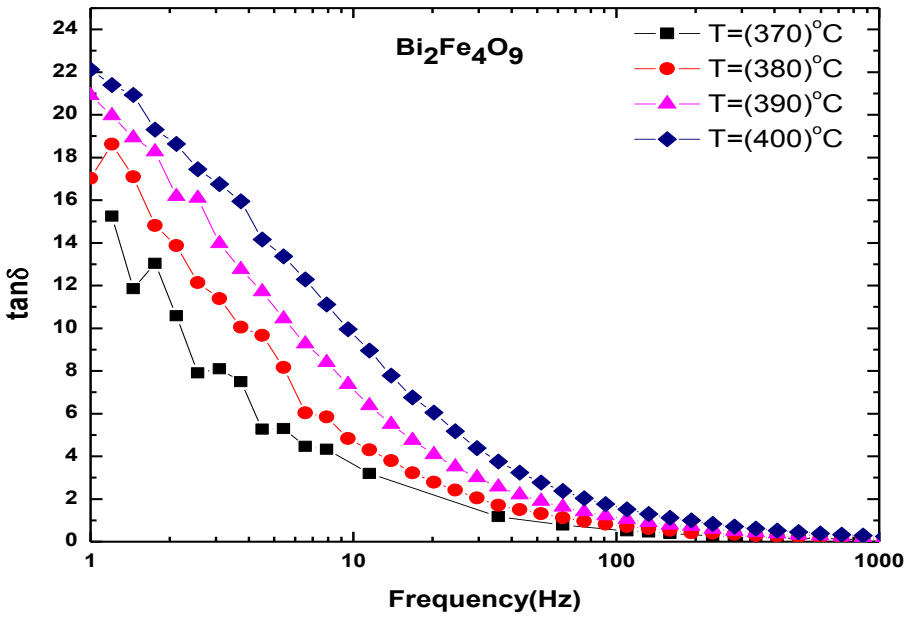

(a)

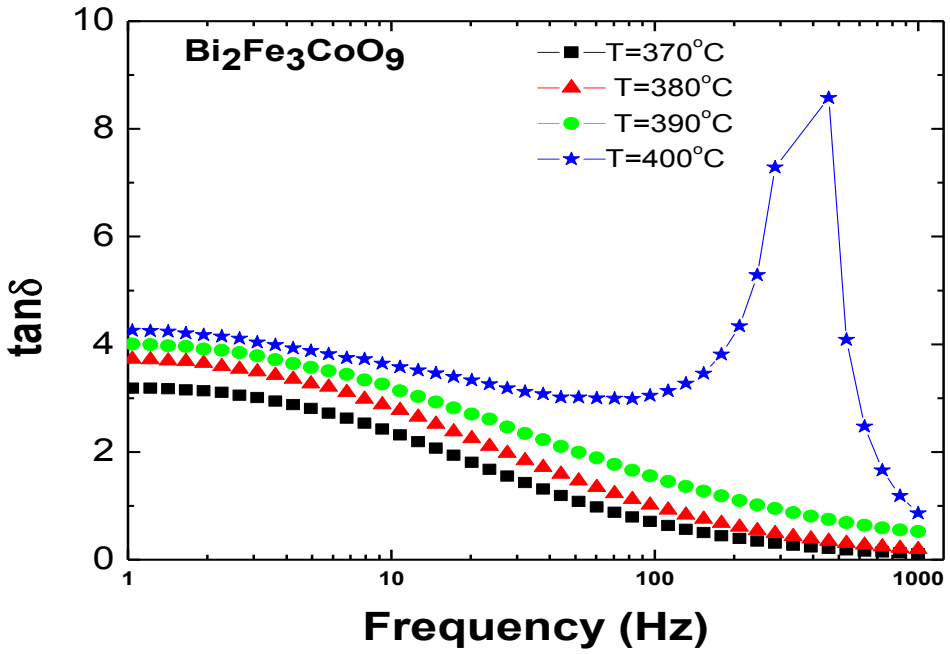

(b)

Fig.22. tanδ as a function of frequency (a) Pure $Bi_2Fe_4O_9$ (b) 20% Co-doped $Bi_2Fe_4O_9$

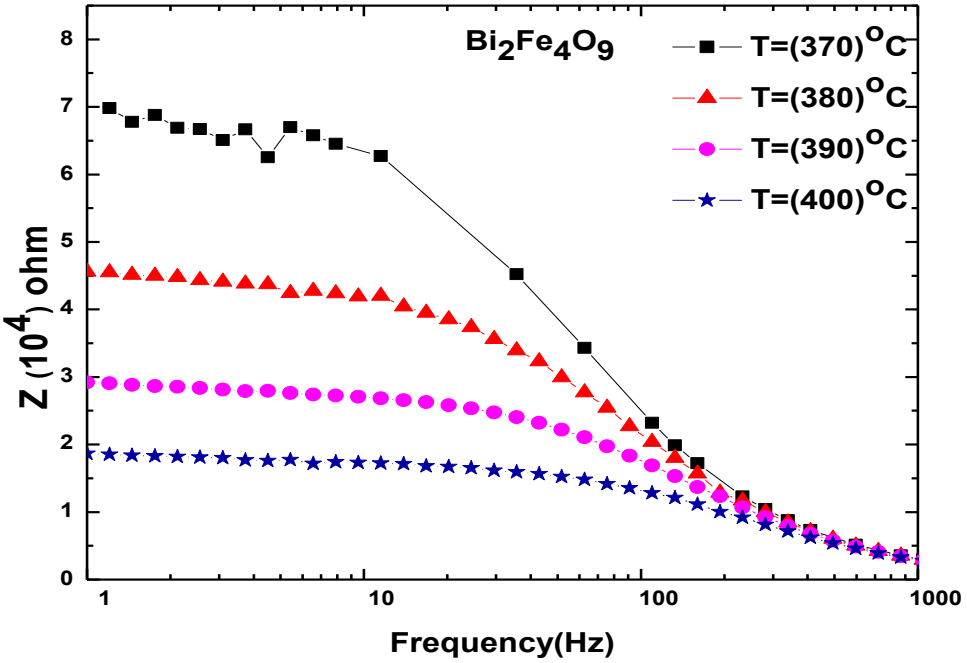

(a)

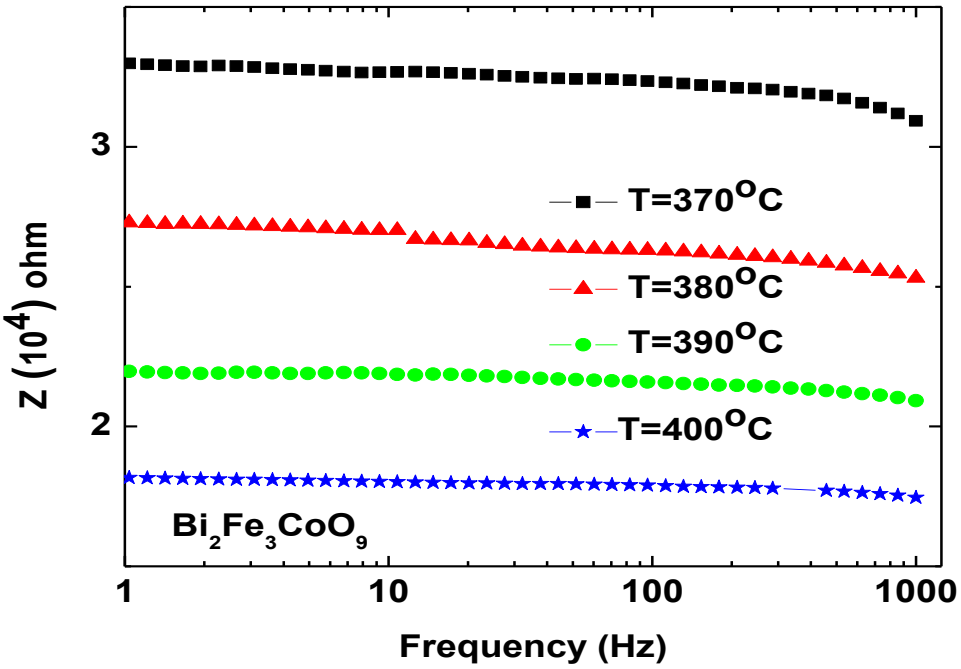

(b)

Fig.23.Impedance as a function of frequency (a) pure $Bi_2Fe_4O_9$ (b)20% Co-doped $Bi_2Fe_4O_9$

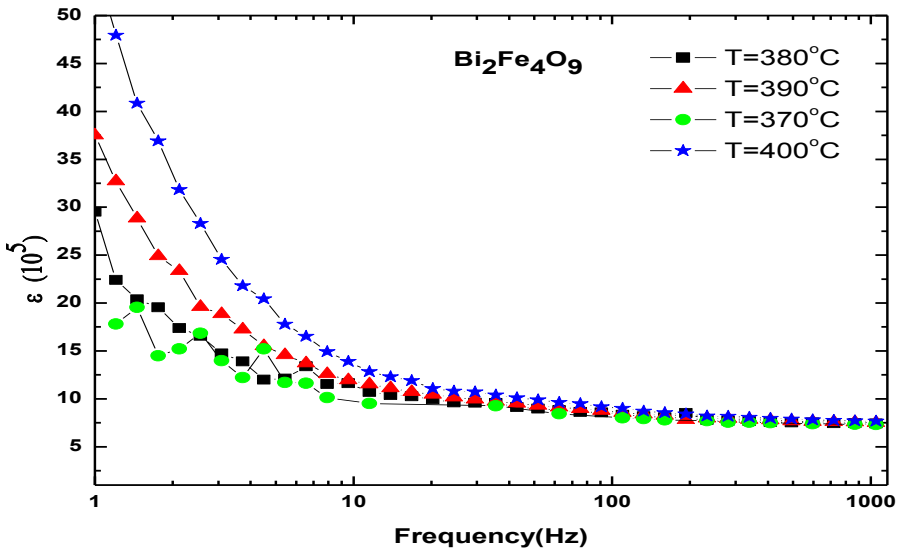

Fig.24.Dielectric constant as a function of frequency of pure $Bi_2Fe_4O_9$

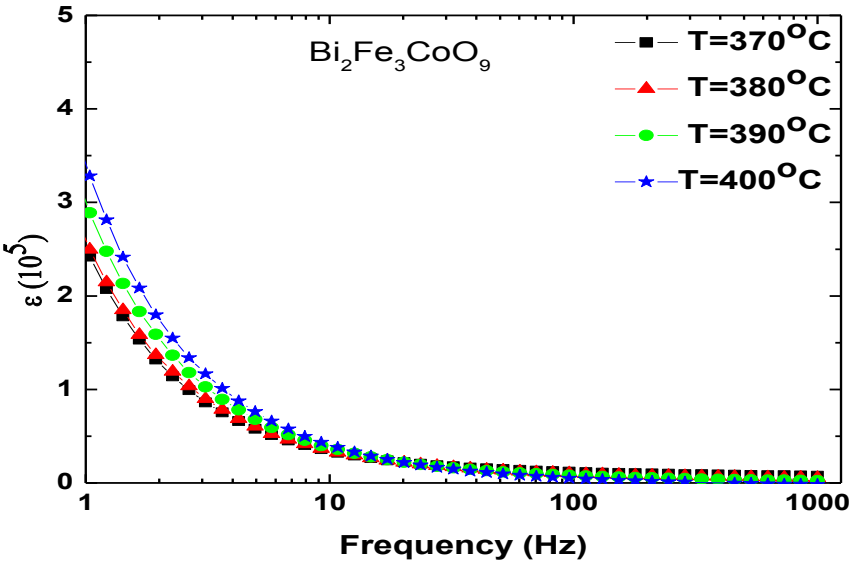

Fig.25.Dielectric constant as a function of frequency of 20% Co-doped $Bi_2Fe_4O_9$

We can see from the plots that tan δ decreases in 20% Co-doped $Bi_2Fe_4O_9$ in comparison to $Bi_2Fe_4O_9$. Impedance as a function of frequency decreases at higher frequencies in $Bi_2Fe_4O_9$ whereas in 20% co-doped $Bi_2Fe_4O_9$ it is constant. Comparison of dielectric constant shows $Bi_2Fe_3CoO_9$ has less dielectric constant than $Bi_2Fe_4O_9$.

(iv) UV-Visible Spectroscopy Analysis

Fig. 26 and fig.27 show the UV-Visible spectra of pure $Bi_2Fe_4O_9$ and 20% Co doped $Bi_2Fe_4O_9$ respectively.

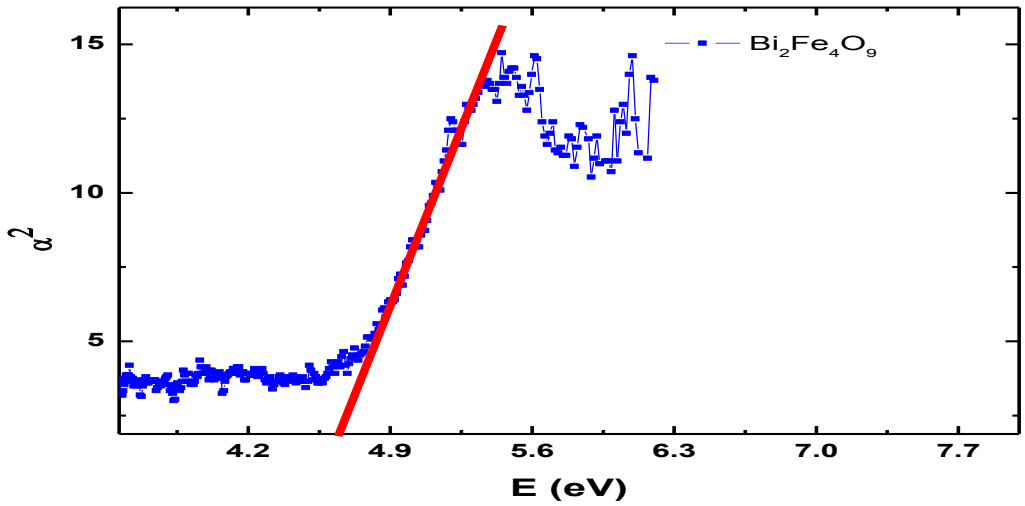

Fig.26. UV-Visible Spectra of Pure $Bi_2Fe_4O_9$

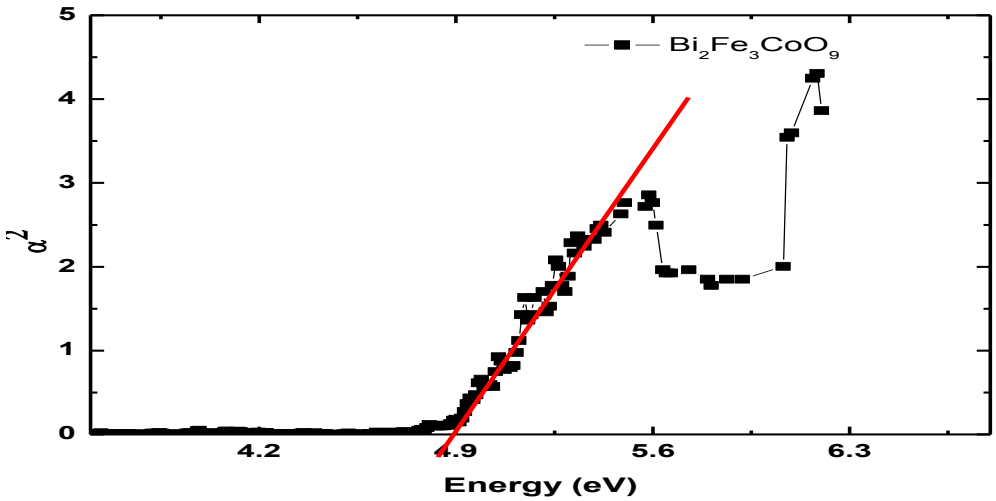

Fig.27.UV-Visible Spectra of 20% Co-doped $Bi_2Fe_4O_9$

We have calculated the band gap energy of $Bi_2Fe_4O_9$ and $Bi_2Fe_3CoO_9$ using the equation which shows the relation between absorption coefficient and band gap energy.

For direct band gap the equation will be

$$\alpha^2 = (h\nu - E_g)^2 \quad \text{Or} \quad \alpha = h\nu - E_g$$

The above equation of "α" is similar to the equation of a straight line where frequency is the variable and band gap energy is comparable with the intercept. Using the above relation it is found that both $Bi_2Fe_4O_9$ and 20% Co-doped $Bi_2Fe_4O_9$ have direct band gap and band gap energy of 4.64 eV and 4.91 eV respectively.

8. Conclusion:

- Most of the major peaks in 20% Co-doped $Bi_2Fe_4O_9$ are in accordance with pure $Bi_2Fe_4O_9$. It is found that with 20% Co doping crystallite size increases than pure $Bi_2Fe_4O_9$.
- 20% Co-doped $Bi_2Fe_4O_9$ shows more porosity than the pure $Bi_2Fe_4O_9$.
- Dielectric property (ε and tanδ)decreases with increase in frequency and it is independent on the temperature at higher frequencies. For a particular frequency and temperature dielectric constant of $Bi_2Fe_4O_9$ is more than $Bi_2Fe_3CoO_9$.
- $Bi_2Fe_4O_9$ and 20% Co-doped $Bi_2Fe_4O_9$ have a direct band gap of band gap energy 4.64 eV and 4.91 eV respectively. The increase in band gap implies the enhancement of dielectric properties.

9. References:

1. **Introduction to solid state physics**,
Charles Kittel, 7th Edition, Willy India Publication.
2. **Spin current and magneto electric effect in no collinear magnets**, Hosho Katsura, Naoto Nagaosa, Alexander and V. Balatsky, Phys. Rev. Lett. **95,** 057205 (2005).
3. **The renaissance of magneto-electric multiferroics**,
Nicola A. Spaldin and Manfred Fiebig, Science **10**, 1114671 (2005).
4. **Spiral magnets as magneto-electrics**
T. Kimura, and Nicola A. Hill, J. Phys. Chem. B.**104**, 6694 (2000)
5. **Classifying multiferroics: Mechanisms and effects**,
Daniel Khomskii, Physikalisches Institute, Universidad zu Köln, Zülpicher Strasse **77**, 50937 (2009)
6. **Magnetic frustration in an iron based Cairo pentagonal lattice**
E. Ressouche, V. Simonet, B. Canals, M. Gospodinov and V. Skumryev, Phys. Rev. Lett.**103**, 267204 (2009)
7. **Phonon and magnon scattering of antiferromagnetic $Bi_2Fe_4O_9$**
M. N. Iliev, A. P. Litvinchuk, and V. G. Hadjiev, Phys. Rev. B.**81**, 024302 (2010).
8. **Why are there so few magnetic ferroelectrics**
Nicola A. Hill, J. Phys. Chem. B.**104**, 6694-6709 (2000).
9. **Substantial magneto electric coupling near room temperature in $Bi_2Fe_4O_9$**
A. K. Singh, S. D. Kausik, Brijesh Kumar and S.Patnaik, Appl. Phy. Lett. **92**, 132910 (2008).
10. **Geometrically frustrated magnetic materials**
John E. Greed an, **10**, 1039 (2000).
11. **Effect of antiferromagnetic order on the dielectric properties of $Bi_2Fe_4O_9$**
Y. A. Park, K. M. Song, K. D. Lee, C. J. Won, and N. Hur, Appl. Phy. Lett. **96,** 092506 (2010)
12. **Synthesis and characterization of $Bi_2Fe_4O_9$ powders**
Jingyoan Zhao, Ting Liu and Yebin Xu, Material Chemistry and Physics, **128**, 338391 (2011).
13. **Multiferroic magneto electric composites: Historical perspective, status, and future directions**,
Ce-Wen Nan, M.I.Bichurin, Shuxiang Dong, J. Appl. Phys. **103**, 031101 (2008)
14. **X-ray reflection in accordance with Bragg's Law**,
http://serc.carleton.edu/research_education/geochemsheets/BraggsLaw.html
15. **Scanning Electron Microscope layout and its functions,**
http://www.ammrf.org.au/myscope/sem/practice/principles/layout.php
16. **UV-Vis Absorption Spectroscopy,**
http://www.p-forster.com/iindex.htm?/english/themes/spectroscopy/basics/UV-Vis%20instrumentation